rings at these positions in the molecule. The $\Delta\sigma$ curves disagree rather strongly near the maximum at $s = 8$ Å^{-1}. In order to fit the experimental curve, two j_2 terms with opposite signs and very different damping factors (λ) are required to eliminate the natural j_2 peak at $s = 8$ Å^{-1}, while the theoretical curve allows the j_2 to reach this maximum. A detailed analysis shows that it is the coupling between the two j_2 terms which generates the two rings in the experimental $\Delta\sigma$ function.

At present, highly accurate differential cross sections can be measured for gaseous targets. With the adoption of the approximation that $\Delta\rho_c \ll 2Z\Delta\rho$ the data can be transformed into charge-density difference functions. A comparison with HF calculations shows good overall agreement with the exception of two weak rings of charge. These rings reflect either the importance of $\Delta\rho_c(r)$ or the influence of the π_g^2, π_u^2 interaction on the bond. However, a configuration interaction calculation should be able to confirm the ring structure in $\Delta\rho$.

†This research was supported by the R. A. Welch Foundation and by the Department of Defense Joint Services Electronics Program through the U. S. Air Force Office of Scientific Research Contract No. F44620-71-C-0091.

*Present address: Naval Research Laboratory, Washington, D. C. 20390.

[1]M. Fink and R. A. Bonham, Rev. Sci. Instrum. 41, 389 (1970).

[2]R. A. Bonham and M. Fink, *High Energy Electron Scattering* (Van Nostrand, New York, 1974), Chap. 3.

[3]M. Fink, P. G. Moore, and D. Gregory, "Precise Determination of Differential Electron Scattering Cross Sections I. The Apparatus and N_2 Results" (to be published).

[4]D. A. Kohl and L. S. Bartell, J. Chem. Phys. 51, 2891 (1969).

[5]M. Naon and M. Cornille, J. Phys. B 5, 1965 (1972).

[6]C. Tavard, Cah. Phys. 20, 397 (1965).

[7]M. Fink, D. A. Kohl, and R. A. Bonham, Chem. Phys. Lett. 4, 349 (1969).

[8]R. F. W. Bader, W. H. Henneker, and P. E. Cade, J. Chem. Phys. 46, 3341 (1967).

Magnetohydrodynamic Properties of the *D*-Shaped Tokamak Controlled by Active Field Shaping

H. Toyama, K. Makishima, H. Kaneko, M. Noguchi, and S. Soshikawa*
Department of Physics, Faculty of Science, University of Tokyo, Tokyo, Japan
(Received 31 December 1975)

By means of active field shaping, a D-shaped, elongated plasma has been obtained with a maximum plasma current of 50 kA corresponding to $q = 2.4$ for the toroidal magnetic field of 2.2 kG. In this stage magnetic perturbations of $m = 2$ kinklike mode have been at high level. The disruptive instability with a negative voltage spike, an expansion of the plasma column, and an inward shift in the major radius have been observed. These magnetohydrodynamic properties are similar to those of circular cross section tokamaks.

Tokamaks with certain noncircular cross sections may introduce significant advantages relative to conventional tokamaks.[1] For an elliptical cross section with toroidal major radius R, major and minor semi-axes b and a, respectively, toroidal field B_t, and total plasma current I_p, the safety factor at the plasma edge, q_a, is

$$q_a = \frac{2\pi a^2 B_t}{\mu_0 R I_p} \frac{1+(b/a)^2}{2}, \quad (1)$$

under the assumption of a flat current profile. With the safety factor, the toroidal magnetic field, the plasma volume, and the aspect ratio R/a fixed, the plasma current and the current density of the elongated tokamak can be larger than those of the circular one by a factor

$$\kappa_1 = (a/b)^{1/3}[1+(b/a)^2]/2, \quad (2)$$

$$\kappa_2 = (a/b)^{2/3}[1+(b/a)^2]/2, \quad (3)$$

respectively. The gross magnetohydrodynamic (MHD) configurational stability in noncircular tokamaks has been studied in devices such as Doublet series,[2] Finger-Ring,[3] and Rector.[4] However, experimental data on the stability at low q in the case of active field shaping are insufficient.

A device named TNT (Tokyo Noncircular Tokamak) using external shaping coils has been constructed to investigate what type of cross section makes best use of the advantages of noncircular

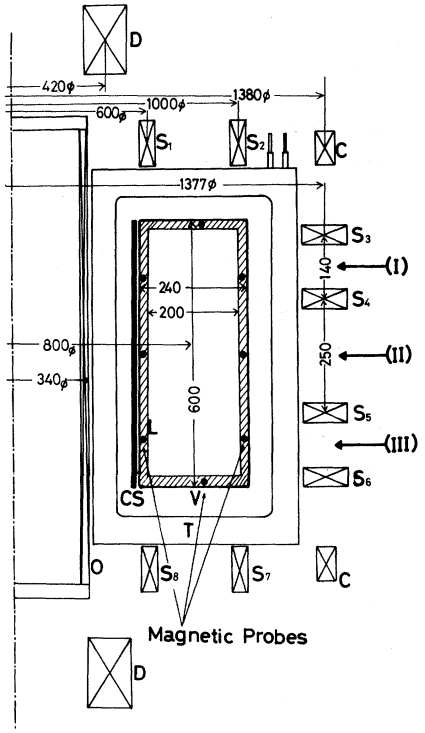

FIG. 1. Cross-sectional view of the TNT machine. T, toroidal coil; O, Ohmic heating coil; S_1–S_8, shaping coils; C, Ohmic-cancelling coil; D, shaping decoupling coil; V, vacuum chamber; L, molybdenum limiter; CS, copper shell; I–III, positions of optical measurements; $Z = 19.5$ cm, O, -19.5 cm. Positions of magnetic probes are shown by black circles. The dimensions are in millimeters.

cross sections. Figure 1 is a cross-sectional view of the TNT. The vacuum chamber is of a rectangular cross section (60 cm high and 24 cm wide) of 6–8-mm-thick stainless steel with gaps so that Ohmic heating field can penetrate. The major radius is $R = 40$ cm. The plasma volume is limited by the molybdenum limiter with a rectangular aperture of $2a = 20$ cm and $2b = 56$ cm. Thus, the degree of elongation $b/a = 2.8$ gives advantage factors of $\kappa_1 = 3.1$ and $\kappa_2 = 2.2$. The 24 toroidal coils, powered by a 130-kJ capacitor bank, provide a maximum toroidal magnetic field of 4.4 kG. The plasma current is driven by an air-core transformer of fifty turns, powered by a 25-kJ capacitor bank. A pair of eight-turn coils are used to cancel the stray magnetic field from the air-core transformer. The external shaping field is provided by eight shaping coils of ten turns each. Besides the strength of the field, the rise time and the shape of the field can be widely altered by use of taps. The shaping

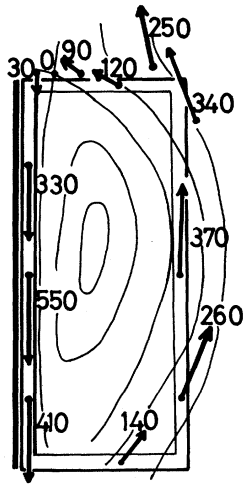

FIG. 2. A typical example of polodial-field measurements in gauss and a rough sketch of the magnetic configuration for the optimized plasma (nearly the current-maximum stage).

coil system is decoupled from the air-core transformer by a pair of forty-turn decoupling coils. The copper shell (10 mm thick) with gaps is placed as an open shell on the inner side of the cross section of the vacuum chamber (see Fig. 1) to restrict the magnetic surface. The vacuum chamber acts as a resistive shell with a time constant of 1 msec. Hydrogen gas is fed pulsively using two fast-acting valves. Filling gas pressure is $(0.7–7.0)\times10^{-4}$ Torr. Preionization is done using a 10-kW rf (800 kHz) oscillator and an electron gun.

The optimization has been carried out as to the maximum plasma current, the discharge duration, and up-to-down symmetry of the plasma, by adjusting turns of each shaping coil and the Ohmic-cancelling coil. The poloidal magnetic field distribution is measured by eight magnetic probes located inside the vacuum chamber as shown in Fig. 1 and two movable magnetic probes outside the vacuum chamber. Figure 2 shows a typical example of poloidal-field measurements and a rough sketch of the magnetic configuration for the optimized plasma 600 μsec after the start of the discharge. Under this optimized condition, each shaping coil, except S_4 and S_5 in Fig. 1, was carrying a total current of 10 kAt. The polarity of the current in each coil was the same and different from that of the coil D. The coils S_4 and S_5 were not used in this case. The probe measurement with no plasma current gave the vertical field of average strength 80 G and the average n index of 0.1, where $n = -(R/B_z)(\partial B_z/\partial R)$.

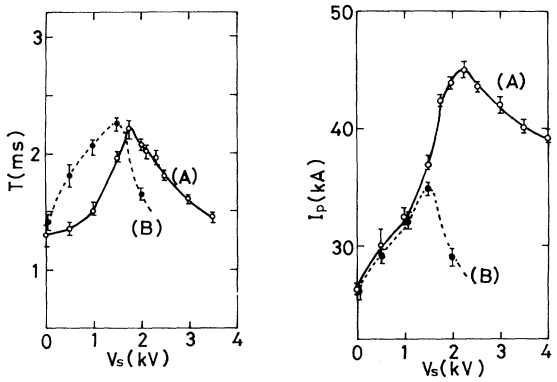

FIG. 3. The discharge duration and the maximum plasma current versus the charging voltage of the capacitor bank for the shaping field. Curve A, $n \approx 0.1$, curve B, $n \approx -0.2$, where $n = -(R/B_z)(\partial B_z/\partial R)$.

It can be inferred that there are two magnetic neutral points at top and bottom, nearly on the outer surface of the vaccum chamber. They stayed almost at rest during the discharge; they were absent with no plasma current. After 1 msec, when the shaping field was dominant, the plasma column was seen to move toward the inner or outer side for nonoptimum shaping field. The optimum shaping field maintained almost the same magnetic configuration throughout the discharge. The effects of the shaping field strength are summarized in Fig. 3 (solid curves). As a comparison, another configuration of the shaping field was examined; i.e., the current and the polarity of the coils S_3–S_6 were the same and other shaping coils were not used ($n \simeq -0.2$, bad curvature). The dotted curves in Fig. 3 correspond to this configuration. In this case the magnetic neutral points moved rapidly toward the center of the plasma at 0.8 msec. These results show that the plasma was actively controlled, and the optimum configuration of the external shaping field could maintain the D-shaped, elongated plasma. The optical measurements were carried out using silicon p-i-n diode detectors at the three positions (I: $z = 19.5$ cm, II: $z = 0$, III: $z = -19.5$ cm) as shown in Fig. 1. The intensity ratio of the the total light from the plasma at the position I to II was 0.7–0.8 throughout the discharge, giving additional evidence for the elongation of the plasma column. A typical example of the optimized discharge is shown in Fig. 4. The current in the primary winding is crowbarred at 1.3 msec. The maximum plasma current was 50 kA corresponding to $q_a = 2.4$ for the toroidal magnetic field of 2.2 kG. The loop voltage at maximum current,

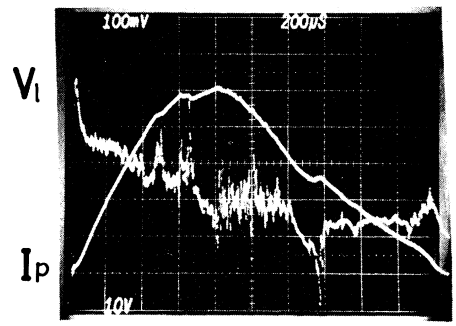

FIG. 4. A typical example of the plasma current I_p (10 kA/div) and the loop voltage V_1 (10 V/div) for $B_t = 2.2$ kG. Time scale is 200 μ sec/div.

15 V, and the current density, 60 A/cm^2, give the resistivity of 1 mΩ cm, which corresponds to the conductivity temperature of about 15 eV. The electron temperature may be higher because of the $I(dL/dt)$ term and the effective Z.

The low-frequency ($f \leq 100$ kHz) MHD oscillations with positive spikes on the loop voltage and dips on the plasma current in current-growing stages (Fig. 4) were studied by eight magnetic probes (Fig. 1). The time evolution of the oscillations are summarized along the trajectory of the discharge in Fig. 5. The mode structure is assumed to be $\exp[i(m\theta + n\varphi)]$, where φ and θ are major and minor azimuthal angles, respectively. The mode rotated in the electron diamagnetic drift direction which is the same as that reported for the ST tokamak,[5] and n was always 1. The $m = 2$ oscillations were at high level near the current maximum and the current was limited at a level corresponding to $q_a \approx 2$, which was practically independent of the Joule-heating electric field.

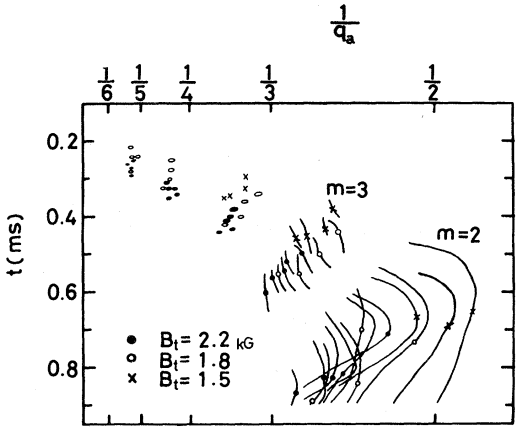

FIG. 5. Time evolution of the kinklike mode instability in the current-growing stage.

The typical frequency of the $m = 2$ mode was 18 kHz. These MHD properties are similar to those of circular tokamaks.[5,6]

If we assume that the major axis of the cross section b is reduced effectively to b' due to current shrinking while a is unchanged and that the $m = 2$ mode is a kink mode,[7] the value of b' can be estimated from Fig. 5 and Eq. (1); the estimated value of b' is 23 cm for $t = 0.8$ msec, giving the elongation degree of 2.3. This is the lower limit since $m = 2$ mode may be (partly or entirely) the resistive tearing mode.[8]

In the latter half of the discharge, there appeared negative voltage spikes (~ -20 V) on the loop voltage (Fig. 4). The magnetic probe signals show the following: (i) These negative spikes occurred when the $m = 2$ oscillations were almost damped down; (ii) these corresponded to the superposition of $m = 0$ expansion in the minor radius and an inward shift in the major radius (~ 2 cm); and (iii) n is 0. An increase of the H_β signal coincided with the negative voltage spike. These observations show that this negative voltage spike is quite similar to the "disruptive instability"[5,9] familiar in circular tokamaks.

Because of lack of direct measurements of temperature and density, definite statements cannot be made about the β value. However, it is demonstrated experimentally that a D-shaped, elongated configuration at low safety factor q has been obtained by means of active field shaping and that the MHD properties of the discharge are analogous to those of a circular cross-section tokamak.

*Present address: Plasma Physics Laboratory, Princeton University, Princeton, N. J. 08540.

[1]T. Ohkawa, Kaku Yugo Kenkyu 20, 557 (1968); D. Dobrott and M. S. Chu, Phys. Fluids 16, 1371 (1973); L. A. Artsimovich and V. D. Shafranov, Pis'ma Zh. Eksp. Teor. Fiz. 15, 72 (1972) [JETP Lett. 15, 51 (1972)].

[2]T. Ohkawa and H. G. Voorhies, Phys. Rev. Lett. 22, 1275 (1969); T. H. Jensen *et al.*, in *Plasma Physics and Controlled Nuclear Fusion Research* (International Atomic Energy Agency, Vienna, 1974), Vol. 1, p. 281.

[3]A. V. Bortnikov *et al.*, in *Proceedings of the Sixth European Conference on Controlled Fusion and Plasma Physics, Moscow, U. S. S. R., 1973* (U. S. S. R. Academy of Sciences, Moscow, 1973), Vol. 1, p. 165, and in *Proceedings of the Third International Symposium on Toroidal Plasma Confinement, Garching, Germany, March 1973* (Max-Planck-Institut für Plasmaphysik, Garching, Germany, 1973), and in *Plasma Physics and Controlled Nuclear Fusion Research* (International Atomic Energy Agency, Vienna, 1974), Vol. 1, p. 147.

[4]U. Ascoli-Bartoli *et al.*, in *Plasma Physics and Controlled Nuclear Fusion Research* (International Atomic Energy Agency, Vienna, 1974), Vol. 1, p. 191.

[5]J. C. Hosea *et al.*, in *Plasma Physics and Controlled Nuclear Fusion Research* (International Atomic Energy Agency, Vienna, 1971), Vol. 2, p. 425.

[6]S. V. Mirnov and I. B. Semenov, At. Energ. 30, 20 (1971) [Sov. At. Energy 30, 22 (1971)]; K. Makishima *et al.*, Phys. Rev. Lett. 36, 142 (1976).

[7]V. D. Shafranov, Sov. Phys. Tech. Phys. 15, 175 (1970); S. Inoue *et al.*, Phys. Lett. 53A, 342 (1975).

[8]H. P. Furth *et al.*, Phys. Fluids 16, 1054 (1973).

[9]L. A. Artsimovich, Nucl. Fusion 12, 215 (1972).

Pulsed Ion Diode Experiment*

D. S. Prono, J. W. Shearer, and R. J. Briggs
Lawrence Livermore Laboratory, University of California, Livermore, California 94550
(Received 2 March 1976; revised manuscript received 24 May 1976)

Ion current densities up to several kiloamperes per square centimeter and total ion currents ranging from 50 to 150 kA have been produced at voltages of 100–300 kV in a modified relativistic-electron-beam diode. The experiments are in general accord with the predictions of a recent reflex-triode theory.

There has been considerable interest recently in the production of intense ion beams with pulsed diode techniques.[1-3] Intense ion flows in the diode regions of electron beam generators have, in fact, been invoked to explain aspects of the observed diode behavior for both self-pinched flows[3] and reflex diode configurations.[2,4-7]

In this Letter, we present results of an experimental study of the ion flow created in the reflex configuration described in Ref. 2. Briefly, this configuration consists of a planar diode immersed in an externally applied axial magnetic field, with a thin anode foil and a virtual cathode beyond the foil that reflects essentially all of the electrons

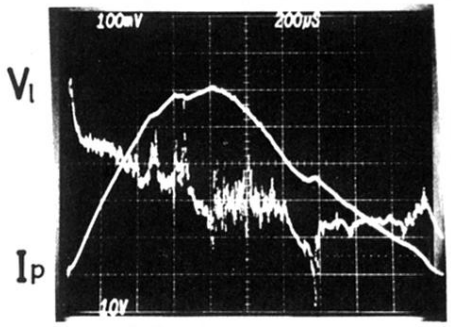

FIG. 4. A typical example of the plasma current I_p (10 kA/div) and the loop voltage V_1 (10 V/div) for B_t =2.2 kG. Time scale is 200 μ sec/div.